Optically directed molecular transport and 3D isoelectric positioning of amphoteric biomolecules

Dean G. Hafeman*†‡, James B. Harkins IV*‡, Charles E. Witkowski II*‡, Nathan S. Lewis§, Robert J. Warmack‡, Gilbert M. Brown‡, and Thomas Thundat‡

*Protein Discovery, Inc., 418 South Gay Street, Knoxville, TN 37902; §Division of Chemistry and Chemical Engineering, California Institute of Technology, 210 Noyes Laboratory, 1200 East California Boulevard, Pasadena, CA 91125; and ‡Oak Ridge National Laboratory, P.O. Box 2008, Oak Ridge, TN 37831

Edited by Calvin F. Quate, Stanford University, Stanford, CA, and approved February 24, 2006 (received for review November 14, 2005)

We demonstrate the formation of charged molecular packets and their transport within optically created electrical force-field traps in a pH-buffered electrolyte. We call this process photoelectrophoretic localization and transport (PELT). The electrolyte is in contact with a photoconductive semiconductor electrode and a counterelectrode that are connected through an external circuit. A light beam directed to coordinates on the photoconductive electrode surface produces a photocurrent within the circuit and electrolyte. Within the electrolyte, the photocurrent creates localized force-field traps centered at the illuminated coordinates. Charged molecules, including polypeptides and proteins, electrophoretically accumulate into the traps and subsequently can be transported in the electrolyte by moving the traps over the photoconductive electrode in response to movement of the light beam. The molecules in a single trap can be divided into aliquots, and the aliquots can be directed along multiple routes simultaneously by using multiple light beams. This photoelectrophoretic transport of charged molecules by PELT resembles the electrostatic transport of electrons within force-field wells of solid-state charge-coupled devices. The molecules, however, travel in a liquid electrolyte rather than a solid. Furthermore, we have used PELT to position amphoteric biomolecules in three dimensions. A 3D pH gradient was created in an electrolyte medium by controlling the illumination position on a photoconductive anode where protons were generated electrolytically. Photoelectrophoretic transport of amphoteric molecules through the pH gradient resulted in accumulation of the molecules at their apparent 3D isoelectric coordinates in the medium.

electrophoresis | light | mass spectrometry | protein transport | proteomics

Several examples of light-directed transport exist. Ashkin *et al.* (1) first used a single light beam to create a force gradient that trapped suspended dielectric particles. This optical trapping technique works optimally for ≈1-μm particles (2). Such devices, commonly called optical tweezers, are quite versatile and additionally have been used to build 3D nanostructures and to control the spinning of trapped particles with optically polarized light (3, 4). In practice, however, optical tweezers cannot transport objects smaller than the wavelength of light. This includes many biomolecules e.g., DNA fragments, oligonucleotides, proteins, and peptides. Instead, such small molecules must first be attached to larger particles called "handles" (5).¶ Another technique, called the "optoelectronic tweezers," has been used to position single particles with intensity-modulated light directed onto a semiconductor electrode (6). This alternative optoelectronic technique utilizes dielectrophoresis wherein the modulated electric field induces transient electrical dipoles in the particles. Both methods, however, are limited to transporting large particles.

We demonstrate light-driven transport of proteins without attachment to larger particles. We use a beam of light directed onto a photoconductive semiconductor surface in contact with an electrolyte medium to create controlled electrical field traps that attract charged molecules in the medium. The force-field traps are created by an electrophoretic photocurrent (dc) focused at the illuminated regions of the semiconductor. Charged molecules in the medium migrate electrophoretically toward, and become trapped in, these high-field regions. Moving the beam of light along the semiconductor surface correspondingly moves the traps and thereby causes translation of the trapped molecules within the medium. We call this process photoelectrophoretic localization and transport (PELT). The light beam and, consequently, the high-field regions in the electrolyte can be redirected in real time so as to dynamically steer the trapped molecules while in transit. We show that biological molecules, such as peptides and proteins, can be transported in such a manner.

Fig. 1 shows the basic components needed for PELT. They include a photoconductive electrode and a counterelectrode connected through an external circuit. Both electrodes are in contact with an electrolyte containing the molecules to be transported. The counterelectrode may be of any geometry, including a small-area electrode, a large conductive surface (shown in Fig. 1), or another photoconductive electrode. We employ a doped semiconductor as a photoconductive electrode and the external circuit to apply a bias voltage between the semiconductor and a counterelectrode made of a platinum wire, wire loop, or foil. The bias voltage creates an electric field that depletes majority charge carriers from a surface layer of the semiconductor in contact with the electrolyte. This electrically insulating depletion layer prevents direct current from flowing across the semiconductor/electrolyte interface in the dark. The depletion layer, however, becomes conductive in regions that are illuminated with photons of energy greater than the band gap of the semiconductor. Even light absorbed at the back surface of the semiconductor can be made to produce photoconductivity within a depletion layer at its front surface provided that the minority carrier lifetime of the photogenerated charge carriers is sufficiently long to permit their diffusion between the two surfaces. In an alternative photovoltaic mode of operation, a "built-in" bias voltage at the semiconductor/electrolyte interface permits the external circuit to be used without the bias

Conflict of interest statement: D.G.H., J.B.H., C.E.W., and N.S.L. own either stock or stock options in Protein Discovery, Inc., which holds a license to a patent application pending in the U.S. Patent Office that may cover portions of the technology described in this paper. G.M.B. and T.T. are listed coinventors on the subject patent application. In addition, R.J.W., G.M.B., and T.T. are employed at the Oak Ridge National Laboratory by its contractor, UT-Battelle, which is the assignee of the subject patent application.

This paper was submitted directly (Track II) to the PNAS office.

Abbreviations: PELT, photoelectrophoretic localization and transport; CCD, charged-coupled device.

†To whom correspondence should be addressed. E-mail: dean@proteindiscovery.com.

¶The optical trapping potential of <1-μm particles is less than their thermal energy at room temperature, i.e., 1/2 kT in each dimension or 3/2 kT in three dimensions, where k is the Boltzman constant (1.38066×10^{-17} J/K) and T is absolute temperature. Consequently, purely optical trapping of molecules may be possible at very low temperatures.

www.pnas.org/cgi/doi/10.1073/pnas.0509881103

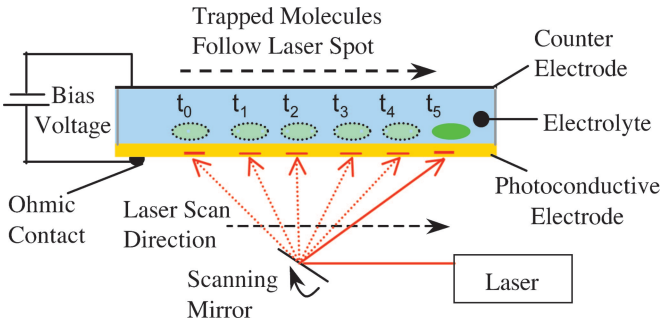

Fig. 1. System for PELT of charged molecules in an electrolyte. A laser beam is used to illuminate a moving spot on a photoconductive electrode. Charged molecules in the electrolyte accumulate in an electric field trap at the illuminated spot. Trapped molecules follow the laser spot over the photoconductive electrode as it moves from its initial position at t_0 to its final position at t_5.

voltage. In this mode, the photons provide all of the energy needed for molecular transport.

In either the photovoltaic or photoconductive modes, a dc faradaic current flows across the semiconductor/electrolyte interface only where the semiconductor is illuminated. Thus a focused spot of light on such an interface generates a localized electrophoretic photocurrent within the electrolyte and consequently, according to Ohm's law, produces a 3D electric field, $\vec{E}$, within the electrolyte:

$$\vec{E} = \rho\vec{j}, \qquad [1]$$

where ρ and $\vec{j}$ are the resistivity and the vectorial current density in the electrolyte medium, respectively. This relationship predicts the electric field to be greatest at regions of highest current density, i.e., at electrolyte regions adjacent to the illuminated semiconductor surface. Such high-field regions within the electrolyte form spatial traps into which molecules of the selected charge migrate electrophoretically. Furthermore, as depicted in Fig. 1, moving the position of the light beam changes the spatial position of an electric field trap and thereby results in transport of charged molecules accumulated within the trap. In addition, we demonstrate that the transported molecules can be partitioned into separate aliquots and separately dispensed at different coordinates in an electrolyte medium.

We further demonstrate that amphoteric molecules (i.e., molecules with both acidic and basic groups, such as peptides and proteins) can be positioned at their 3D isoelectric coordinates within a pH-buffered electrolyte medium. This molecular positioning is accomplished by using photoelectrolysis to create a 3D pH gradient in an aqueous pH-buffered medium. The pH gradient can be precisely created and positioned by controlling the illumination intensity, duration, and position on a photoconductive surface immersed in the medium. Subsequent electrophoretic transport of the amphoteric molecules through the pH gradient results in their concentration at their respective 3D isoelectric coordinates.

Results and Discussion

Fig. 2 is a fluorescence intensity image of fluorescently labeled BSA accumulated into an ≈1-mm diameter electrical field trap in aqueous 250 mM histidine on a TiO_2 semiconductor photoanode. The Alexa-Fluor-488-labeled BSA ($BSA_{AlexaFluor488}$) sample was applied in an ≈5-mm diameter spot and photoconcentrated by PELT to an ≈1-mm diameter, or 1/25th of the original sample area.

Fig. 3 shows the time course of the differential transport by PELT of two oppositely charged proteins in the pH 7.8 histidine electrolyte [cytochrome *c*, pI = 9.6; and Marina-blue-labeled

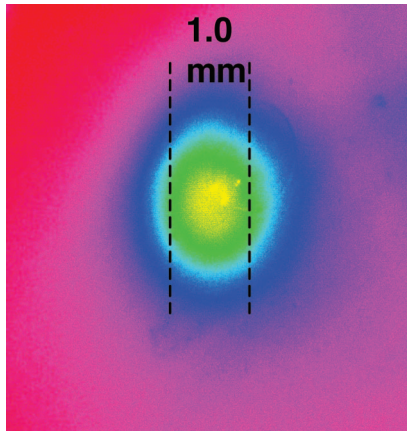

Fig. 2. Fluorescence intensity image of $BSA_{AlexaFluor488}$ photoconcentrated by PELT. The fluorescent protein was concentrated into an illuminated electric field trap region in an aqueous electrolyte in contact with a thick-film TiO_2 photoanode. The TiO_2 was biased at 1.5 V (vs. Pt) and illuminated for 10 min with an ≈1-mm beam of a 325-nm He–Cd laser. The fluorescence image was obtained by excitation with a standard near-UV lamp. The $BSA_{AlexaFluor488}$ is seen as a bright yellow spot in the (false color) intensity image centered at the laser spot.

BSA ($BSA_{MarinaBlue}$), pI ≈ 4.9]. The two proteins were introduced into liquid agarose and allowed to solidify as a single sample spot, ≈3 mm in diameter. Differential transport and separation of the two proteins was accomplished by PELT with an n-type germanium (Ge) photoanode. The transport process is shown in side-by-side white light and fluorescence images recorded at 10-min intervals. A 1-mW HeNe laser beam was initially positioned ≈2 mm to the right of the sample spot and then was moved periodically to stay just in front of the leading edge of the $BSA_{MarinaBlue}$ fluorescence. The negatively charged $BSA_{MarinaBlue}$, when transported by PELT in this manner, appeared as a focused fluorescent spot moving toward the laser-illuminated position on the Ge photoanode. In contrast, positively charged cytochrome *c* moved away from the original sample spot as a "diffuse cloud," driven by electrophoresis in the opposite direction toward a platinum wire counterelectrode.‖

The photoconductive electrodes used for PELT also can be used to generate a 3D pH gradient within the transporting medium. Protons are generated by oxidation of water at a photoanode according to

$$H_2O \rightarrow 2H^+ + 1/2\ O_2 + 2e^-. \qquad [2]$$

Conversely, protons are consumed by reduction of water at a photocathode according to

$$2H_2O + 2\ e^- \rightarrow 2\ OH^- + H_2. \qquad [3]$$

A spatially localized pH gradient, therefore, is generated at any illuminated point on the surface of a current-carrying photoanode or photocathode in a pH-buffered electrolyte.

Because of the pH gradient, amphoteric molecules closely approach, but do not contact, the surface of the photoelectrodes under the PELT transport conditions reported here. This phenomenon was observed most clearly in PELT experiments with relatively long illumination periods and with electrolytes having

‖The mechanism of PELT is unique in that molecules are transported within focused free-energy wells. In contrast, by conventional electrophoresis, molecules follow the continuous lines of electric flux to destination electrodes. Conventional electrophoresis would be equivalent to PELT in the special case where an attracting electrode is moved sequentially just in front of the attracted molecules.

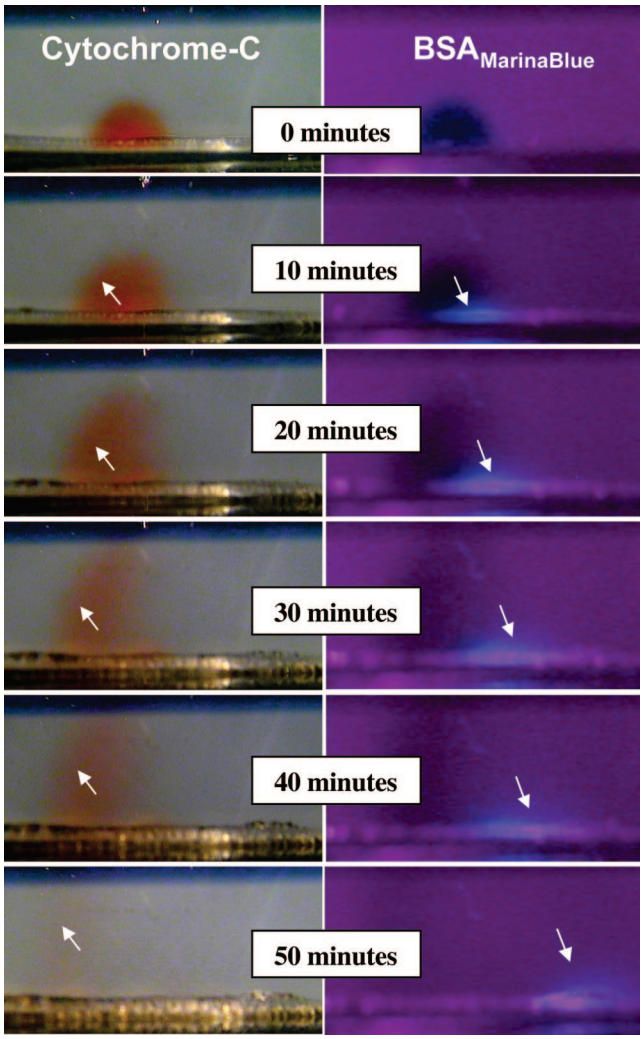

Fig. 3. Time course of fluorescent $BSA_{MarinaBlue}$ separation from oppositely charged cytochrome *c* by PELT. (*Right*) Fluorescence of the $BSA_{MarinaBlue}$ taken with near-UV illumination. (*Left*) White-light photos that reveal the position of cytochrome *c*. The arrows indicate the direction of transport for each of the two proteins as seen in a side view through a transparent chamber filled with aqueous electrolyte (and 1% agarose to prevent convection). At the base of the chamber is a Ge photoanode; a Pt wire counterelectrode is present at the upper left corner. A mixture of the two proteins initially was deposited at a central spot close to the base. Separation of the two proteins was effected by periodically moving the center of a 543-nm (green) HeNe, 1-mm diameter laser spot on the photoanode to keep it ≈2 mm to the right of center of the $BSA_{MarinaBlue}$ fluorescence. (The green laser was turned off to make the photographs.) The (light blue) fluorescence of $BSA_{MarinaBlue}$ is seen to be increasing in intensity as the negatively charged BSA is transported by PELT (to the right) as a focused spot away from fluorescence-quenching cytochrome *c*. The positively charged cytochrome *c*, in contrast, is seen to be migrating toward the negatively charged counterelectrode in a diffuse (non-PELT) manner.

relatively low buffer capacity. As observed by fluorescence microscopy (side view), negatively charged $BSA_{AlexaFluor488}$ (in 50 mM histidine, pH 7.8, electrolyte) initially concentrated into an apparent "isoelectric zone" ≈1 mm above an illuminated spot on a positively charged Ge photoanode. During subsequent continuous illumination of the same spot, the fluorescent $BSA_{AlexaFluor488}$ molecules reversed their direction and then moved successively farther away from the photoanode surface. After 10 min of pH relaxation in the dark, however, the molecules were again attracted toward the same illumination spot (but as observed previously, reversed their direction upon continued stationary illumination). Apparently, once the amphoteric protein molecules are attracted into an isoelectric zone above the illuminated photoanode, they acquire a total charge of zero and stop migrating toward the illumination spot. After prolonged illumination, however, (and generation of more acid at the illumination spot) the surface pH apparently drops farther and the initially attracted (negatively charged) proteins then acquire a positive charge and begin to move away from the illuminated photoanode. A series of experiments showed that increasing the pH-buffering capacity in the electrolyte allowed the $BSA_{AlexaFluor488}$ to more closely approach the illuminated surface. Conversely, focusing of the light to a smaller spot (to increase the current density) resulted in increasing the width of depletion of protein from the surface at any given prolonged illumination time. Thus, proteins could be brought to specified distances above the illuminated electrode surface by manipulation of the current density, illumination dwell time, and pH buffer capacity.**

In contrast to stationary illumination, continuous or step-wise lateral movement of the light beam over the Ge photoanode surface causes continued translation of the amphoteric $BSA_{AlexaFluor488}$ molecules in the direction of translation of the light beam. Upon repositioning of the light beam to a new spot on the photoanode, the molecules again moved toward the new spot, even after prolonged illumination of the previous spot (i.e., after they presumably had reached their isoelectric coordinates). Movement of the light beam, however, changes the coordinates where protons are generated, and the pH in a previously illuminated region relaxes toward the bulk pH by diffusion. Thereby amphoteric molecules at their isoelectric coordinates are able to regain charge and migrate toward the new position of the light beam.

Fig. 4 demonstrates dynamic "steering" of a mixture of stained proteins in aqueous histidine electrolyte with 1% agarose on a Ge photoanode. The electrical mobility of proteins was further increased by adding 1% SDS to the sample.†† The proteins were first accumulated from a larger (3 mm) spot (in 4 μl of sample) into a smaller (1 mm) spot by illumination of the photoanode for 5 min. Next, the light beam was sequentially repositioned in a counterclockwise pattern in 2-mm steps at 5-min intervals. In response to each repositioning step, all of the proteins in the mixture followed the laser spot, migrating as a single packet of charged molecules. Each protein was stained a different color so that if separation had occurred, it would have been observed readily.

Fig. 5 shows that the protein sample could be photoelectrophoretically divided into two aliquots and the two aliquots transported independently within separate force field traps. Similar to the procedure used in Fig. 4, the sample mixture was first accumulated into a smaller spot by PELT. The laser beam then was split into two equivalent illumination spots (of equal light intensity, duration, and diameter) on the photoanode by time-division multiplexing (cycling at 2 Hz). The two illuminating laser spots were spaced 3 mm apart, resulting in division of the protein mixture into two corresponding aliquots, one centered on each laser spot. The distance between the laser spots was increased by ≈3 mm at 5-min intervals with the result that the distance between protein aliquots also increased by the same distance. Each protein aliquot followed only the closest laser spot, as predicted from Eq. **1**, because the vectorial current density, $\vec{j}$, falls off rapidly with the distance *r* from the center of

**Ampholyte buffers near their isoelectric point provide both low conductivity (minimizing joule heating) and relatively high buffering capacity. Examples and their isoelectric points are histidine (pH 7.8), glutamic acid (pH 3.1), and aspartic acid (pH 3.0).

††Negatively charged SDS binds to proteins so that their isoelectric points are shifted to a much lower pH. Thus, at neutral pH, they all migrate in the same direction with a significantly greater electrical mobility.

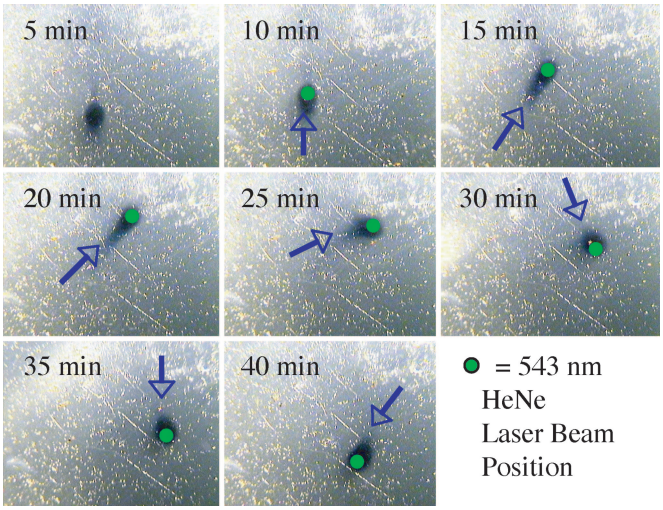

Fig. 4. Dynamic steering of transported proteins by PELT. The sample contains a mixture of seven stained proteins in SDS applied in Tris-glycine electrolyte containing 1% agarose (to prevent convection). A 1-mW, 543-nm HeNe laser beam 1 mm in diameter was projected through the sample to direct protein transport over a Ge photoanode. After concentration by PELT for 5 min, the protein mixture appears as a blue spot that is slightly larger than the laser spot. Subsequently, the center of the laser spot was repositioned to ≈2 mm from the center of the protein spot in the direction indicated by the arrow. (The location of each repositioned laser spot is shown as a green dot.) Five minutes after each repositioning, the protein mixture was again found to be recentered over the laser spot (see Movie 1, which is published as supporting information on the PNAS web site).

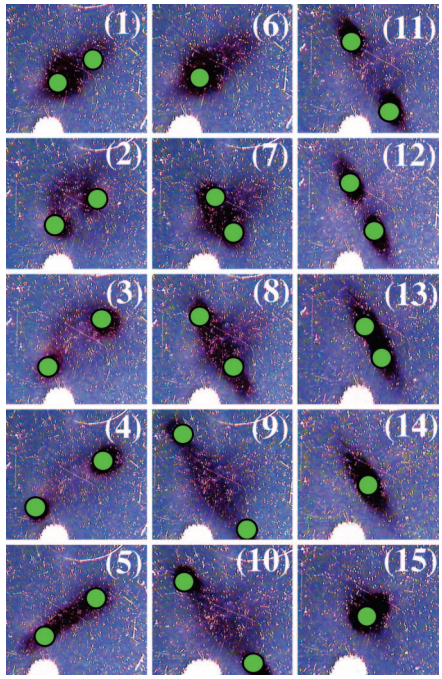

Fig. 5. Division of a protein mixture into two aliquots by PELT. The stained protein sample was first concentrated by PELT (with the HeNe laser beam) into a 1-mm-diameter spot on a Ge photoanode. Subsequently, the laser light was divided by equal time-division multiplexing of a single beam at 2 Hz into two laser spots (seen as green dots) centered 3 mm apart. The dark-blue protein spot then began to separate into two spots (frame 1). After 5 min, the protein sample appeared as two separate aliquots, one centered at each laser spot (frame 2). The laser beams then were repositioned twice the distance apart, ≈1.5 mm in front of the protein spot centers. After 5 min, the aliquot separation distance increased to the new distance between laser spots (frame 3). The laser repositioning procedure was repeated until a final separation distance of ≈1 cm was achieved for the protein aliquots (frame 4). The illumination sequence then was reversed (frames 5 and 6) to recombine the aliquots into a single spot (frame 7). Next, the procedure was repeated, dividing the laser beam in an orthogonal direction, with the result that two new aliquots were formed in the orthogonal direction (frames 8–10). Then the procedure was again reversed to bring the proteins back together as a single spot at the origin (frames 11–15). The protein composition of the two aliquots appeared to be virtually identical, judging from the similar coloration of the two spots (all proteins together in the mixture appear blue) (see Movie 2, which is published as supporting information on the PNAS web site). The large white spot, white arcs, and small spots seen in the photographs are artifacts from specular reflection and from light scattering by scratches and other defects on the Ge surface.

a trap (e.g., as $\approx 1/r^2$ from a point current source on a large area planar electrode). After the two protein aliquots were separately transported, they were next recombined into a single spot at the origin. The separation, transport, and recombination cycle for the aliquots was then repeated in an orthogonal direction. All transport and molecular steering steps were accomplished simply by moving the light beam without physically repositioning electrodes.

Similar to the way that electrons are transported in solid-state charge-coupled devices (CCDs), ions in electrolytes are transported by PELT as packets of charge. In CCDs, packets of electronic charge are contained within electrostatic "wells" of a semiconductor solid and are transferred by shifting the position of the wells (by charging the appropriate electrostatic electrodes in a counterelectrode array) (7). In the case of PELT, packets of ions are transported in electrolytes within free energy wells that are created electrophoretically with the aid of a photoelectrode and a directed light beam.[‡‡] Another feature of PELT, analogous to CCD behavior, is that there is a maximum translational velocity of the free energy wells beyond which the molecules in them (or electrons in CCDs) fail to keep up. For example, at room temperature, the mobility of electrons in silicon is $\approx 1.5 \times 10^3$ cm^2/V·s (7), whereas the electrophoretic mobility of small singly charged polypeptides in water is $\approx 1.5 \times 10^{-4}$ cm^2/V·s (8).[§§] Thus, molecules in water are seven orders of magnitude slower than electrons in silicon. Electrons are transferred 10 μm across gates of CCDs in ≈ 1 ns, whereas translation of polypeptides the same distance in water under the same electric field would take ≈10 ms.

The time (t) required for translation of molecules over any arbitrary distance, x_a, can be calculated as follows, where the mean electrophoretic velocity (dx_a/dt) of the molecules is given as

$$dx_a/dt = \mu \cdot V_p/x_e, \qquad [4]$$

where μ is their electrical mobility, and where V_p and x_e are the applied voltage and effective distance between anode and cathode, respectively. Accordingly, the predicted time required for translation by PELT over the distance x_a is

$$t = x_a \cdot x_e/(V_p \cdot \mu). \qquad [5]$$

For example, with 2 V applied to an illuminated photoanode and a counterelectrode spaced 0.3 cm from the illuminated spot, polypeptides with a single charge would be predicted to require ≈300 s (or 5 min) to traverse a lateral distance of 0.3 cm. In other

[‡‡] In principle, arrays of separately addressable electrodes could be used to transport molecules without the use of light. An array of anodes could be used to transport negatively charged molecules (and an array of cathodes could be used to transport positively charged molecules). See ref. 13 for an example of electrode arrays.

[§§] The mobility of a singly charged small peptide is approximately half the mobility of a doubly charged fluorescein molecule.

words, the proteins predictably should fall behind the trap if it were translated faster than 10 μm/sec under these conditions. This prediction is consistent with the behavior observed in Figs. 4 and 5, in which the proteins remained focused within traps translated ≈0.3 cm in 5 min, (i.e., 10 μm/s). In similar experiments, with the same proteins and conditions, we found that translation of the proteins by PELT fell off sharply when the mean velocity of the light beam exceeded 10 μm/s.[¶¶] Thus, the observed results closely match those predicted by calculation.

To test for protein degradation during translation over photoanodes, human insulin and ubiquitin were translated by PELT under conditions similar to those described for Fig. 3. The proteins then were collected and subjected to MALDI mass spectrometry. No mass peaks were observed other than those of the intact proteins. Both the low voltage (<2 V) dropped across the electrode/electrolyte interface and the fact that amphoteric protein molecules approach but do not appear to contact the photoelectrode surface during transport may contribute to the observed protein stability.

The PELT technique should be useful to transport biomolecules other than proteins, including oligonucleotides, DNA, and RNA. Fixed electrodes were used in previous studies to direct electrophoretic transport of oligonucleotides and to promote hybridization of target oligonucleotides to complementary strands immobilized on the electrodes (9, 10). In addition, Hayward *et al.* (11) electrophoretically assembled charged polystyrene particles (2 μm in diameter) into a patterned array by using a stationary light beam directed through a photomask onto a dc-biased semiconducting thin film. Gurtner *et al.* (12) extended this dc technique to promote DNA hybridization to complementary strands located at an illuminated silicon photoanode. The previous studies, together with the results presented here, suggest that PELT will be useful in the transportation of a variety of biomolecules in addition to proteins.

Within small aqueous volumes, PELT may allow the manipulation of selected single molecules. The use of multiple electric field traps might then allow the manipulation of the single molecules with respect to each other. The limit for confining nonamphoteric charged molecules to small electrophoretic traps in aqueous electrolytes is the larger of two variables: the illumination spot diameter and the diffusion length of the photoexcited charge carriers within the photoconductive electrode. Because illumination of very small spots on semiconductors with short minority-carrier diffusion lengths (7) is feasible, the controlled transport of single molecules by PELT over the same small distances should be as well.

Other possible applications of PELT include electrochromatographic separations and manufacturing of DNA and RNA microarrays. For example, synthesis of specific DNA and RNA sequences has been programmed by controlling pH-dependent electrochemical reactions at prefabricated metal electrode arrays (13). Light-addressable photoanodes used for PELT may be able to accomplish this task less expensively and with more versatility.

In summary, we describe the creation of dynamically changing electrical force field traps in an aqueous electrolyte by using a moving beam of light directed onto a photoconductive electrode in contact with the electrolyte. The process requires a counterelectrode and a faradaic photocurrent within the electrolyte. Packets of charged biological molecules within the electrolyte accumulate in the traps and are transported by moving the light beam. The magnitude, shape, and sign of the force field traps can be controlled by selecting the light intensity, photoconductive electrode material, and the potential applied between the electrodes. We show that PELT can be used to transport polypeptides and proteins in aqueous electrolytes and should be applicable to the transport of any charged molecule (including oligonucleotides, DNA, and RNA). In contrast to the action of optical and optoelectronic tweezers (2–5), small molecules need not be attached to large particle handles for transport by PELT. Potential applications for PELT include electrochromatographic separations, the manufacturing of biochemical microarrays, and the transport, reaction, and assembly of polymeric materials (including nanostructures) in microreaction volumes.

Materials and Methods

TiO_2 thick-film photoanodes were screen-printed 6 μm thick onto fluorine-doped indium-tin-oxide (ITO)-coated float glass (Pilkington, Merseyside, U.K.) and heated at 450°C for 45 min in air to remove organic binder. A copper wire was attached to the ITO coating with silver epoxy resin. The TiO_2 semiconductor films have a band gap of 3.05 eV, thus requiring light wavelengths of ≤370 nm for photoconductivity. (See refs. 14–17 for a discussion of metal oxide semiconductors and their development for solar cell applications.) Protein samples were contained in a transparent polycarbonate cylinder (1.7-cm diameter and 2 cm tall) placed onto the TiO_2 working electrode. Low-electroendosmotic agarose (catalog no. A-6013, Sigma) at 1% in aqueous, 250 mM histidine, pH 7.8 (277 μS/cm conductivity), electrolyte was heated to melting and poured to a 4-mm-deep layer over the TiO_2. A 3-μl hemispherical depression, molded while the agarose was still melted, served as a sample well. The transparent cylinder was topped off with electrolyte (without agarose), and a 3-mm-diameter Pt loop counterelectrode was inserted to ≈4 mm from the TiO_2 surface. $BSA_{AlexaFluor488}$ was diluted into the electrolyte with 20% glycerol, and a 2-μl aliquot having a barely discernable yellow color from the Alexa Fluor label was placed in the sample well. The *N*-hydroxysuccinimide esters of Alexa Fluor 488 and Marina Blue were obtained from Molecular Probes and were used to fluorescently label proteins according to the manufacturer's instructions. Alexa Fluor 488 remains fluorescent at pH <4.0 so that it can be visualized under low pH conditions generated near photoanode surfaces. For protein photoconcentration, the TiO_2 film was illuminated through the ITO-coated glass with an ≈1-mm-diameter, 325-nm He–Cd, 10-mW laser light beam. During laser illumination, a bias potential of 1.5 V was applied to the TiO_2 relative to a Pt counterelectrode. Illumination of TiO_2 through the ITO glass rather than the sample (*i*) avoided photobleaching of fluorescent proteins, (*ii*) increased the photoefficiency (photocurrent/light power ratio) by ≈50%, and (*iii*) caused less degradation of the TiO_2 film with intense illumination.

Ge photoanodes (Polishing Corporation of America, Santa Clara, CA) were n-type, 508 cm in diameter, and 0.036 cm thick, with 0.4-Ω·cm resistivity, and they were (100) oriented. A eutectic mixture of In–Ga was worked with a metal scribe into a 0.5-cm^2 ohmic contact area of Ge. A copper lead was then attached with silver epoxy. The light source for use with Ge photoanodes was a 543-nm (green) JDS Uniphase (Milpitas, CA) HeNe laser, model 1101P, with an actual power output of 1 mW at 543 nm. The laser beam was directed through the electrolyte and sample, creating a spot 1 mm in diameter on the photoanode. The beam was positioned with motor-controlled mirrors controlled by the LABVIEW (National Instruments, Austin, TX) program.

A PELT transport chamber for the experiments shown in Fig. 3 was made from a glass cylinder (45 mm in diameter, 5 mm in length) placed onto the Ge photoanode. The 1% agarose in

[¶¶]The viscosity of water limits PELT velocity. Light-directed transport in rarified media, e.g., air or vacuum, hypothetically could be much faster. The counter-charges in such media, however, would be ''image'' charges on the semiconductor electrode. The density of transported molecules, therefore, would be limited by the space-charge density within the semiconductor depletion layer (on the order of 1 fmol of charges per squared millimeter). Thus, the number of charges per packet would be much smaller in such media, but the transport velocity would be much greater.

aqueous histidine electrolyte was melted and used to cover the photoanode to a depth of 3 mm, and 2 μl of a mixture containing cytochrome *c* and Marina-Blue-labeled BSA ($BSA_{MarinaBlue}$) in the electrolyte (each at $\approx$1 mg/ml) was pipetted gently into the liquid agarose. The agarose was allowed to solidify, and the chamber was filled with additional electrolyte. A platinum wire counterelectrode was lowered into the electrolyte buffer to a position $\approx$3 mm to the left and 3 mm above the initial position of the protein sample seen in Fig. 3. A Model 273 EG&G Princeton Applied Research potentiostat/galvanostat run in the galvanostat mode was set to -0.5 mA. The laser spot was centered $\approx$2 mm to the right of the $BSA_{MarinaBlue}$ spot and re-adjusted at 5-min intervals to remain there while the $BSA_{MarinaBlue}$ was transported by PELT.

For the experiments shown in Figs. 4 and 5, the PELT chamber was made by similarly pouring melted 1% agarose in Tris-glycine electrolyte buffer [63 mM Trizma base (catalog no. T-6066, Sigma)/6 mM glycine (catalog no. G-8898, Sigma), pH 8.6] into a 1/8 inch $\times$ 1.5 inch O-ring on a Ge photoanode. A 3-μl hemispherical depression in the agarose served as a sample well. A polystyrene cylinder (2 cm in diameter) was placed onto the agarose to serve as chamber walls and was subsequently topped off with electrolyte without agarose. A mixture of seven stained proteins with SDS detergent (Kaleidoscope, catalog no. 161-0324, Bio-Rad) and 20% glycerol comprised the protein sample, 2 μl of which was layered under the electrolyte in the sample well. A counterelectrode made from a platinum loop (1 cm in diameter) was submerged in the top electrolyte so that the distance from the Ge photoanode was $\approx$3 mm. The Ge photoanode was biased at +1 V with respect to Pt. The applied protein mixture was first concentrated to a 1.5-mm-diameter spot from an original sample spot 3 mm in diameter by illumination for 5 min with the laser beam (1 mm in diameter) directed to the center of the protein sample.

We thank Dr. Ring-Ling Chen for assistance and advice in construction of experimental equipment; Dr. Rubye Farahi for assistance in preparation of thin-film materials; Dr. Greg Hurst for assistance with MALDI mass spectrometry; and Drs. Kilian Dill, Bruce Jacobsen, Evelyn McGown, David Hachey, Richard Caprioli, Alfred Yergy, and Michael Sailor for helpful advice and assistance. This work was conducted under a cooperative research and development agreement between UT-Battelle and Protein Discovery, Inc., and was supported by National Institute on Drug Abuse Small Business Innovation Research Contract N43DA-3-7735 (to Protein Discovery, Inc.). In addition, partial support was received from the U.S. Department of Energy Office of Biological and Environmental Research and Environmental Management Science Program (T.T.). Oak Ridge National Laboratory is managed by UT-Battelle for the U.S. Department of Energy under contract DE-AC05-00OR22725.

1. Ashkin, A., Dziedzic, J. M., Bjorkholm, J. E. & Chu, S. (1986) *Optics Lett.* **11,** 288–290.
2. Molloy, J. E. & Padgett, M. J. (2002) *Contemp. Phys.* **43,** 241–258.
3. MacDonald, M. P., Paterson, L., Volke-Sepulveda, K., Arlt, J., Sibbett, W. & Dholakia, K. (2002) *Science* **296,** 1101–1103.
4. Friese, M. E. J., Nieminen, T. A., Heckenberg, N. R. & Rubinsztein-Dunlop, H. (1998) *Nature* **394,** 348–350, and erratum (1998) **395**, 621.
5. Hirano, K., Baba, Y., Matsuzawa, Y. & Mizuno, A. (2002) *Appl. Phys. Lett.* **80,** 515–517.
6. Chiou, P. Y., Ohta, A. T. & Wu, M. C. (2005) *Nature* **436,** 370–372.
7. Sze, S. M. (1981) in *Physics of Semiconductor Devices* (Wiley, New York), 2nd Ed., pp. 407–430.
8. Manz, A., Effenhauser, C. S., Burggraf, N., Harrison, D. J., Seiler, K. & Fluri, K. (1994) *J. Micromech. Microeng.* **4,** 257–265.
9. Heller, M. J. (1996) *IEEE Eng. Med. Biol. Mag.* **March/April,** 100–103.
10. Cheng, J., Sheldon, E. L., Wu, L., Uribe, A., Gerrue, L. O., Carrino, J., Heller, M. J. & O'Connell, J. P. (1998) *Nat. Biotechnol.* **16,** 541–546.
11. Hayward, R. C., Saville, D. A. & Aksay, I. A. (2000) *Nature* **404,** 56–59.
12. Gurtner, C., Edman, C. F., Formosa, R. E. & Heller, M. J. (2000) *J. Am. Chem. Soc.* **122,** 8589–8594.
13. Oleinikov, A. V., Gray, M. D., Zhao, J., Montgomery, D. D., Ghindilis, A. L. & Dill, K. (2003) *J. Proteome Res.* **2,** 313–319.
14. Tan, M. X., Laibinis, P. E., Nguyen, S. T., Kesselman, J. M., Stanton, C. E. & Lewis, N. S. (1994) *Prog. Inorg. Chem.* **41,** 21–144.
15. Khan, S. U. M., Al-Shahry, M. & Ingler, W. B., Jr. (2002) *Science* **297,** 2243–2245.
16. Lewis, N. S. (2001) *Nature* **414,** 589–590.
17. Hagfeldt, A. & Gratzel, M. (2000) *Acc. Chem. Res.* **33,** 269–277.